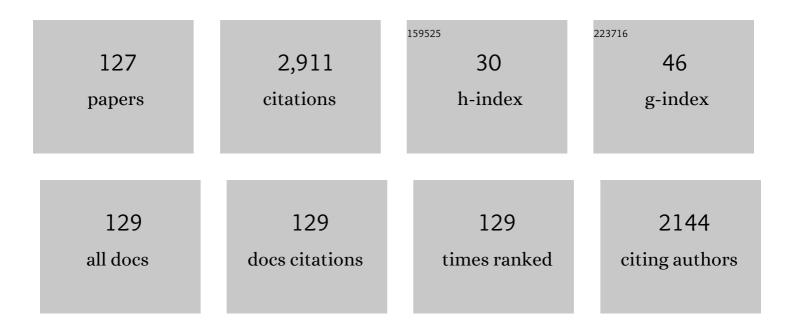
## Li-Bing Liao

List of Publications by Year in descending order

Source: https://exaly.com/author-pdf/149582/publications.pdf Version: 2024-02-01



#	Article	IF	CITATIONS
1	A novel single-composition trichromatic white-emitting Sr3.5Y6.5O2(PO4)1.5(SiO4)4.5 : Ce3+/Tb3+/M phosphor: synthesis, luminescent properties and applications for white LEDs. Journal of Materials Chemistry C, 2014, 2, 1619.	n2+ 2.7	175
2	High Performance Composite Polymer Electrolytes for Lithiumâ€lon Batteries. Advanced Functional Materials, 2021, 31, 2101380.	7.8	151
3	Anchoring Fe <sub>3</sub> O <sub>4</sub> Nanoparticles on Carbon Nanotubes for Microwave-Induced Catalytic Degradation of Antibiotics. ACS Applied Materials & Interfaces, 2018, 10, 29467-29475.	4.0	83
4	Mechanism and process of methylene blue degradation by manganese oxides under microwave irradiation. Applied Catalysis B: Environmental, 2014, 160-161, 211-216.	10.8	73
5	A novel single-phase white light emitting phosphor Ca <sub>9</sub> La(PO <sub>4</sub> ) <sub>5</sub> (SiO <sub>4</sub> )F <sub>2</sub> :Dy <sup>3+</sup> : synthesis, crystal structure and luminescence properties. RSC Advances, 2016, 6, 24577-24583.	1.7	69
6	Study on the adsorption properties of methyl orange by natural one-dimensional nano-mineral materials with different structures. Scientific Reports, 2021, 11, 10640.	1.6	69
7	Luminescence properties and energy transfer in La6Ba4(SiO4)6F2:Ce3+,Tb3+ phosphors. Journal of Luminescence, 2014, 145, 65-70.	1.5	67
8	Structure, luminescence property and energy transfer behavior of color-adjustable La5Si2BO13:Ce3+,Mn2+ phosphors. RSC Advances, 2014, 4, 7288.	1.7	67
9	A novel apatite, Lu <sub>5</sub> (SiO <sub>4</sub> ) <sub>3</sub> N:(Ce,Tb), phosphor material: synthesis, structure and applications for NUV-LEDs. Physical Chemistry Chemical Physics, 2016, 18, 15545-15554.	1.3	65
10	Luminescence investigations of novel orangeâ€red fluorapatite <scp>KL</scp> aSr <sub>3</sub> ( <scp>PO</scp> <sub>4</sub> ) <sub>3</sub> F: Sm <sup>3+</sup> phosphors with high thermal stability. Journal of the American Ceramic Society, 2017, 100, 2221-2231.	1.9	63
11	Strategy for realizing ratiometric optical thermometry via efficient Tb3+-Mn2+ energy transfer in novel apatite-type phosphor Ca9Tb(PO4)5(SiO4)F2. Journal of Alloys and Compounds, 2019, 770, 1237-1243.	2.8	58
12	Photoluminescence properties and energy transfer of Ba <sub>2</sub> Lu(BO <sub>3</sub> ) <sub>2</sub> Cl : Eu <sup>2+</sup> /Eu <sup>3+</sup> ,Tb <sup> Journal Physics D: Applied Physics, 2012, 45, 015302.</sup>	3-tt<\$sup>	ph <b>s</b> phors.
13	Comparative Investigation of Green and Red Upconversion Luminescence in <scp><scp>Er</scp></scp> 3+ Doped and <scp><scp>Yb</scp></scp> 3+/ <scp>Er</scp> 3+Codoped La <scp>OC</scp> 1. Journal of the American Ceramic Society, 2012, 95, 3229-3234.	1.9	55
14	Color-tunable photoluminescence phosphors of Ce3+ and Tb3+ co-doped Sr2La8(SiO4)6O2 for UV w-LEDs. Journal of Solid State Chemistry, 2015, 225, 149-154.	1.4	55
15	Influence of interlayer cations on organic intercalation of montmorillonite. Journal of Colloid and Interface Science, 2015, 454, 1-7.	5.0	45
16	A novel inorganic thermal insulation material utilizing perlite tailings. Energy and Buildings, 2019, 190, 25-33.	3.1	45
17	Novel emission-tunable oxyapatites-type phosphors: Synthesis, luminescent properties and the applications in white light emitting diodes with higher color rendering index. Dyes and Pigments, 2017, 139, 361-371.	2.0	44
18	Ca9La(PO4)5(SiO4)Cl2:Dy3+: A white-emitting apatite-type phosphor pumped for n-UV w-LEDs. Journal of Luminescence, 2017, 181, 407-410.	1.5	44

#	Article	IF	CITATIONS
19	Preparation, crystal structure and luminescence properties of a novel single-phase red emitting phosphor CaSr <sub>2</sub> (PO <sub>4</sub> ) <sub>2</sub> :Sm <sup>3+</sup> ,Li <sup>+</sup> . RSC Advances, 2019, 9, 4834-4842.	1.7	44
20	Dysprosium doped novel apatite-type white-emitting phosphor Ca 9 La(PO 4 ) 5 (GeO 4 )F 2 with satisfactory thermal properties for n -UV w -LEDs. Dyes and Pigments, 2017, 139, 180-186.	2.0	43
21	Structure and photoluminescence properties of red-emitting apatite-type phosphor NaY9(SiO4)6O2:Sm3+ with excellent quantum efficiency and thermal stability for solid-state lighting. Scientific Reports, 2017, 7, 15171.	1.6	37
22	Multi-color luminescence evolution and efficient energy transfer of scheelite-type LiCaGd(WO4)3:Ln3+ (Ln = Eu, Dy, Tb) phosphors. Ceramics International, 2019, 45, 1837-1845.	2.3	37
23	Synthesis, broad-band absorption and luminescence properties of blue-emitting phosphor Sr8La2(PO4)6O2:Eu2+ for n-UV white-light-emitting diodes. Ceramics International, 2014, 40, 13709-13713.	2.3	36
24	Synthesis and characterization of Mn intercalated Mg-Al hydrotalcite. Journal of Colloid and Interface Science, 2016, 479, 115-120.	5.0	35
25	Fabrication of Fe-doped birnessite with tunable electron spin magnetic moments for the degradation of tetracycline under microwave irradiation. Journal of Hazardous Materials, 2017, 338, 428-436.	6.5	35
26	A novel reddish-orange fluorapatite phosphor, La6-Ba4(SiO4)6F2: xSm3+ - Structure, luminescence and energy transfer properties. Journal of Alloys and Compounds, 2018, 757, 79-86.	2.8	35
27	Color tunable emission and energy transfer of Ce 3+ and Tb 3+ co-doped novel La 6 Sr 4 (SiO 4 ) 6 F 2 phosphors with apatite structure. Materials Research Bulletin, 2015, 72, 245-251.	2.7	34
28	Synthesis, structure and green luminescence evolution of apatite-type Sr3.5Y6.5O2(PO4)1.5(SiO4)4.5:Eu2+,Tb3+ phosphors. Journal of Luminescence, 2014, 156, 49-54.	1.5	33
29	Synthesis, photoluminescence properties and energy transfer behavior of color-tunable fluorapatite phosphor Sr9Gd(PO4)5(SiO4)F2:Tb3+/Sm3+. Ceramics International, 2016, 42, 16579-16583.	2.3	32
30	Synthesis and tunable luminescence properties of Eu2+ and Tb3+-activated Na2Ca4(PO4)3F phosphors based on energy transfer. Journal of Luminescence, 2013, 135, 20-25.	1.5	31
31	A bifunctional hierarchical porous kaolinite geopolymer with good performance in thermal and sound insulation. Construction and Building Materials, 2020, 251, 118888.	3.2	31
32	Structure and fluorescent properties of Ba 3 Sc(PO 4 ) 3 :Sm 3+ red-orange phosphor for n -UV w-LEDs. Chemical Physics Letters, 2016, 653, 212-215.	1.2	30
33	Tunable luminescence properties and energy transfer of Ba3NaLa(PO4)3F:Tb3+,Sm3+ phosphors with apatite structure. Journal of Luminescence, 2016, 169, 739-743.	1.5	30
34	Structure and luminescence properties of La <sub>6</sub> Ba <sub>4</sub> (SiO <sub>4</sub> ) <sub>6</sub> F <sub>2</sub> :Dy <sup>3+</sup> phosphor with apatite structure. RSC Advances, 2018, 8, 38883-38890.	1.7	29
35	Ultrathin Si/CNTs Paper-Like Composite for Flexible Li-Ion Battery Anode With High Volumetric Capacity. Frontiers in Chemistry, 2018, 6, 624.	1.8	29
36	Synthesis of birnessite with adjustable electron spin magnetic moments for the degradation of tetracycline under microwave induction. Chemical Engineering Journal, 2017, 326, 329-338.	6.6	28

#	Article	IF	CITATIONS
37	Color-tunable luminescence properties and energy transfer of Tb3+/Sm3+ co-doped Ca9La(PO4)5(SiO4)F2 phosphors. Optics and Laser Technology, 2019, 111, 191-195.	2.2	27
38	Luminescence properties and energy transfer of Ce3+/Tb3+ co-doped Ca9La(PO4)5(SiO4)F2 phosphor. Optics Communications, 2015, 335, 90-93.	1.0	26
39	Crystal structure and luminescence properties of novel Sr10â~ (SiO4)3(SO4)3O:xEu2+ phosphor with apatite structure. Ceramics International, 2016, 42, 11687-11691.	2.3	26
40	High Thermal Stability Apatite PhosphorsÂCa2La8(SiO4)6O2:Dy3+/Sm3+ for White Light Emission: Synthesis, Structure, Luminescence Properties and Energy Transfer. Scientific Reports, 2019, 9, 15509.	1.6	26
41	Color-tunable photoluminescence and energy transfer properties of single-phase Ba10(PO4)6O:Eu2+, Mn2+ phosphors. Journal of Solid State Chemistry, 2015, 232, 102-107.	1.4	25
42	High Energy Density Aqueous Liâ€Ion Flow Capacitor. Advanced Energy Materials, 2017, 7, 1601248.	10.2	24
43	Anti-Defect engineering toward high luminescent efficiency in whitlockite phosphors. Chemical Engineering Journal, 2022, 434, 134652.	6.6	24
44	Synthesis and up-conversion luminescence properties of Ho3+, Yb3+ co-doped BaLa2ZnO5. Journal of Physics and Chemistry of Solids, 2015, 83, 152-156.	1.9	23
45	Structure refinement and luminescence properties of a novel apatite-type compound Mn2Gd8(SiO4)6O2. Dyes and Pigments, 2017, 140, 87-91.	2.0	22
46	A novel phosphor of Eu3+-activated Na3GaF6: Synthesis, structure, and luminescence properties. Journal of Luminescence, 2018, 203, 391-395.	1.5	22
47	Synthesis and energy transfer studies of Eu2+ and Mn2+ co-doped Sr3.45Y6.5O2(PO4)1.5(SiO4)4.5 phosphor. Optics Communications, 2013, 309, 64-67.	1.0	21
48	Mineralogical and chemical characteristics of a powder and purified quartz from Yunnan Province. Open Geosciences, 2016, 8, 606-611.	0.6	21
49	Intense broad-band absorption and blue-emitting Ca9La(PO4)5(SiO4)Cl2:Eu2+ phosphor under near-ultraviolet excitation. Journal of Luminescence, 2019, 206, 154-157.	1.5	21
50	Facile combustion synthesis and photoluminescence properties of Ce3+ doped Sr2La8(SiO4)6O2 phosphors. Optical Materials, 2015, 42, 553-555.	1.7	20
51	Crystal structure, thermally stability and photoluminescence properties of novel Sr10(PO4)6O:Eu2+ phosphors. Journal of Solid State Chemistry, 2015, 226, 107-113.	1.4	20
52	Improvement of performance of foam perlite thermal insulation material by the design of a triple-hierarchical porous structure. Energy and Buildings, 2019, 200, 21-30.	3.1	20
53	Luminescence properties of Ca0.65La0.35F2.35:Yb3+, Er3+ with enhanced red emission via upconversion. Materials Research Bulletin, 2011, 46, 543-546.	2.7	19
54	Flexible and high capacity lithium-ion battery anode based on a carbon nanotube/electrodeposited nickel sulfide paper-like composite. RSC Advances, 2017, 7, 49739-49744.	1.7	19

#	Article	IF	CITATIONS
55	Facile Controlled Synthesis of Spinel LiMn2O4 Porous Microspheres as Cathode Material for Lithium Ion Batteries. Frontiers in Chemistry, 2019, 7, 437.	1.8	19
56	Optimization of thermal insulation performance of porous geopolymers under the guidance of thermal conductivity calculation. Ceramics International, 2020, 46, 16537-16547.	2.3	19
57	Luminescence properties and energy transfer investigations of Ba <sub>2</sub> La <sub>2.85â^`x</sub> Tb <sub>0.15</sub> Eu <sub>x</sub> (SiO <sub>4</sub> ) <sub>3</sub> F multicolor phosphor. RSC Advances, 2018, 8, 27332-27341.	1.7	18
58	Color-tunable properties and energy transfer in Ba3GdNa(PO4)3F:Eu2+, Tb3+ phosphor pumped for n-UV w-LEDs. Optics and Laser Technology, 2015, 74, 6-10.	2.2	17
59	Controllable adjustment of the crystal symmetry of K–MnO <sub>2</sub> and its influence on the frequency of microwave absorption. RSC Advances, 2016, 6, 58844-58853.	1.7	17
60	Structure and luminescence properties of Sr9La(PO4)5(SiO4)F2:Dy3+ single-component white-emitting phosphor for n-UV w-LEDs. Optical Materials, 2018, 84, 689-693.	1.7	17
61	Effective Degradation of Rh 6G Using Montmorillonite-Supported Nano Zero-Valent Iron under Microwave Treatment. Materials, 2018, 11, 2212.	1.3	15
62	Enhanced Degradation of Rh 6G by Zero Valent Iron Loaded on Two Typical Clay Minerals With Different Structures Under Microwave Irradiation. Frontiers in Chemistry, 2018, 6, 463.	1.8	15
63	Synthesis of Ce-doped Mn3Gd7â^'xCex(SiO4)6O1.5 for the enhanced catalytic ozonation of tetracycline. Scientific Reports, 2019, 9, 18734.	1.6	15
64	Tunable high-performance microwave absorption for manganese dioxides by one-step Co doping modification. Scientific Reports, 2016, 6, 37400.	1.6	14
65	Structures and luminescent properties of single-phase La 5.90â^'x Ba 4+x (SiO 4 ) 6âr'x (PO 4 ) x F 2 :0.10Ce 3+ phosphors. Journal of Luminescence, 2016, 172, 191-196.	1.5	14
66	Tetrahedral substitution to induce tunable luminescent properties in apatite structural solid-solution phosphors Ca 9 La(PO 4 ) 5 [(Si,Ge)O 4 ]F 2 :Ce 3+. Dyes and Pigments, 2017, 145, 514-517.	2.0	14
67	The Interactions Between Three Typical PPCPs and LDH. Frontiers in Chemistry, 2018, 6, 16.	1.8	13
68	Manganese oxide – an excellent microwave absorbent for the oxidation of methylene blue. RSC Advances, 2015, 5, 55595-55601.	1.7	12
69	Effects of variables on the dispersion of cationic–anionic organomontmorillonites and characteristics of Pickering emulsion. RSC Advances, 2016, 6, 9678-9685.	1.7	12
70	Structure and luminescence properties of multicolor phosphor Ba2La3(SiO4)3Cl:Tb3+,Eu3+. Journal of Solid State Chemistry, 2019, 280, 121009.	1.4	12
71	Luminescence properties and energy transfer of K <sub>3</sub> LuF <sub>6</sub> :Tb <sup>3+</sup> ,Eu <sup>3+</sup> multicolor phosphors with a cryolite structure. RSC Advances, 2019, 9, 4295-4302.	1.7	12
72	Structure and luminescence properties of multicolor phosphor Ba <sub>2</sub> La <sub>3</sub> (GeO <sub>4</sub> ) <sub>3</sub> F:Tb <sup>3+</sup> ,Eu <sup>3+</sup> . RSC Advances, 2019, 9, 35717-35726.	1.7	12

#	Article	IF	CITATIONS
73	A novel blue-purple Ce3+ doped whitlockite phosphor: Synthesis, crystal structure, and photoluminescence properties. Journal of Rare Earths, 2021, 39, 621-626.	2.5	12
74	Intercalation and configurations of organic dye acridine orange in a high-charge montmorillonite as influenced by dye loading. Desalination and Water Treatment, 2014, 52, 7323-7331.	1.0	11
75	Sorptive Removal of Color Dye Safranin O by Fibrous Clay Minerals and Zeolites. Advances in Materials Science and Engineering, 2020, 2020, 1-12.	1.0	11
76	Correlation between intrinsic dipole moment and pyroelectric coefficient of Fe-Mg tourmaline. International Journal of Minerals, Metallurgy and Materials, 2014, 21, 105-112.	2.4	10
77	The influences of Mg intercalation on the structure and supercapacitive behaviors of MoS2. Journal of Materials Science, 2019, 54, 13247-13254.	1.7	10
78	Synthesis of a Novel Catalyst MnO/CNTs for Microwave-Induced Degradation of Tetracycline. Catalysts, 2019, 9, 911.	1.6	10
79	Computational analysis of apatite-type compounds for band gap engineering: DFT calculations and structure prediction using tetrahedral substitution. Rare Metals, 2021, 40, 3694-3700.	3.6	10
80	Tunable upconversion luminescence and energy transfer process between Yb3+ and Er3+ in the CaY4F14. Journal of Luminescence, 2013, 133, 226-229.	1.5	9
81	Synthesis and luminescence properties of Eu2+-activated phosphor Ba3LaK(PO4)3F for n-UV white-LEDs. Polyhedron, 2016, 119, 223-226.	1.0	9
82	Effect of emulsification processes on the stability of Pickering emulsions stabilized by organomontmorillonites. Journal of Dispersion Science and Technology, 2017, 38, 1030-1034.	1.3	9
83	High thermal stability pyroxene type CaScAlSiO6:Tb3+/Sm3+ ceramics with excellent cryogenic optical thermometry performance. Ceramics International, 2022, 48, 4675-4685.	2.3	9
84	Improvement of durability of porous perlite geopolymer-based thermal insulation material under hot and humid environment. Construction and Building Materials, 2021, 313, 125417.	3.2	9
85	Cation-intercalation and conversion-type cathode materials for rechargeable aluminum batteries. Materials Chemistry Frontiers, 2022, 6, 280-296.	3.2	9
86	Electrodeposition of platinum on tourmaline and application as an electrocatalyst for oxidation of methanol. Ionics, 2010, 16, 33-38.	1.2	8
87	Photoluminescence properties and energy transfer behavior of Eu2+/Tb3+ co-doped Ba3Sc(PO4)3 phosphors. Ceramics International, 2015, 41, 14698-14702.	2.3	8
88	Studies on Ce3+ positions and photoluminescence properties of La1.45Ce0.05Ba3.5(SiO4)1.5(PO4)1.5F phosphor. Journal of Luminescence, 2016, 178, 1-5.	1.5	8
89	Fabrication of AO/LDH fluorescence composite and its detection of Hg2+ in water. Scientific Reports, 2017, 7, 13414.	1.6	8
90	Effect of ionic substitution (Ca/Sr/Ba) on structure and luminescent properties of Ce3+ doped fluorapatite. Journal of Luminescence, 2018, 196, 285-289.	1.5	8

#	Article	IF	CITATIONS
91	Fabrication of an AMC/MMT Fluorescence Composite for its Detection of Cr(VI) in Water. Frontiers in Chemistry, 2018, 6, 367.	1.8	8
92	Effects of Nonâ€lonic Surfactants on the Rheological, Electrical and Electrochemical Properties of Highly Loaded Silicon Suspension Electrodes for Semiâ€Solid Flow Batteries. ChemElectroChem, 2020, 7, 3623-3631.	1.7	8
93	Preparation, structure and up-conversion luminescence properties of novel cryolite K3YF6:Er3+, Yb3+. RSC Advances, 2020, 10, 1658-1665.	1.7	8
94	Synthesis and up-conversion luminescence properties of a novel K3ScF6: Yb3+, Tm3+ material with cryolite structure. Journal of Luminescence, 2020, 224, 117285.	1.5	8
95	A new expansion material used for roof-contacted filling based on smelting slag. Scientific Reports, 2021, 11, 2607.	1.6	8
96	Structure, optical characteristics and temperature sensing performance studies of Cs3YF6: Er3+, Yb3+ up-conversion material with cryolite structure. Journal of Solid State Chemistry, 2022, 306, 122720.	1.4	8
97	Influence of different exchangeable cations (Li <sup>+</sup> , Na <sup>+</sup> and Ca <sup>2+</sup> ) on the modification effects and properties of organomontmorillonites used in oil-based drilling fluids/muds. RSC Advances, 2015, 5, 90281-90287.	1.7	7
98	Hydrogeochemistry of Groundwater and Arsenic Adsorption Characteristics of Subsurface Sediments in an Alluvial Plain, SW Taiwan. Sustainability, 2016, 8, 1305.	1.6	7
99	Crystal structure and up-conversion luminescence properties of K3ScF6:Er3+,Yb3+ cryolite. Journal of Alloys and Compounds, 2020, 848, 156336.	2.8	7
100	Structure and luminescence properties of a novel broadband green-emitting oxyapatite-type phosphor. RSC Advances, 2020, 10, 11608-11614.	1.7	7
101	Influence of dysprosium concentration on sensitivity of luminescent thermometers of phosphors Ca9Tb(PO4)5(SiO4)F2. Journal of Rare Earths, 2021, 39, 946-951.	2.5	7
102	Novel Dy3+-doped Ge4+-substituted apatite-type phosphors, Ca9La(PO4)5[(Si1-Ge O4)]F2:Dy3+: Synthesis, structure, crystal chemical features, and luminescent properties. Ceramics International, 2021, 47, 23300-23308.	2.3	7
103	Preparation, crystal structure and photoluminescence properties of novel red-emitting phosphor Mg3Gd2Ge3O12: RE3+ (RE=Sm, Eu) with high thermal stability. Journal of Luminescence, 2021, 240, 118414.	1.5	7
104	Novel apatite KLaSr <sub>3</sub> (PO <sub>4</sub> ) <sub>3</sub> F:Eu <sup>2+</sup> phosphors: synthesis, structure, and luminescence properties. Journal of Materials Research, 2016, 31, 3489-3497.	1.2	6
105	Cobalt Oxide Porous Nanofibers Directly Grown on Conductive Substrate as a Binder/Additive-Free Lithium-Ion Battery Anode with High Capacity. Nanoscale Research Letters, 2017, 12, 302.	3.1	6
106	Experimental Studies on Chemical Activation of Cementitious Materials from Smelting Slag of Copper and Nickel Mine. Materials, 2019, 12, 303.	1.3	6
107	Nanotubular Polyaniline/Reduced Graphene Oxide Composite Synthesized from a Natural Halloysite Template for Application as a High Performance Supercapacitor Electrode. ChemistrySelect, 2022, 7, .	0.7	6
108	A novel Eu <sup>2+</sup> /Tb <sup>3+</sup> coâ€doped phosphor with pyroxene structure applied for cryogenic thermometric sensing. Journal of the American Ceramic Society, 2022, 105, 2903-2913.	1.9	6

#	Article	IF	CITATIONS
109	Mössbauer spectroscopic study of Fe-Mg tourmalines with different Fe contents. Science China Earth Sciences, 2012, 55, 1489-1493.	2.3	5
110	Nanosized Zinc Sulfide/Reduced Graphene Oxide Composite Synthesized from Natural Bulk Sphalerite as Good Performance Anode for Lithium-Ion Batteries. Jom, 2020, 72, 4505-4513.	0.9	5
111	Inorganic thermal insulation material prepared from pitchstone. Journal of Building Engineering, 2020, 32, 101745.	1.6	5
112	Crystal structure and luminescence properties of a novel cryolite-type K3LuF6:Ce3+ phosphor. Journal of Solid State Chemistry, 2019, 277, 32-36.	1.4	4
113	Cation and polyhedron substitution strategies: Effects on local crystal structure and on Bi3+ and Eu3+ co-doped inverse garnet phosphors' luminescence property. Ceramics International, 2022, 48, 12281-12290.	2.3	4
114	Composition Determination and Cathodoluminescence of Natural Apatite from Different Phosphate Deposits in Northern China. Jom, 2014, 66, 992-997.	0.9	3
115	Hydrochemistry of hot springs in geothermal fields of central, northern, and northeastern Taiwan: implication on occurrence and enrichment of arsenic. Environmental Earth Sciences, 2016, 75, 1.	1.3	3
116	Rietveld Structure Refinement of Cu-Trien Exchanged Nontronites. Frontiers in Chemistry, 2018, 6, 558.	1.8	3
117	Mineralogical characteristics of bentonites occurring in Ningcheng and Jianping area, China. Science China Earth Sciences, 2010, 53, 541-549.	2.3	2
118	Using Ionic Liquid Modified Zeolite as a Permeable Reactive Wall to Limit Arsenic Contamination of a Freshwater Lake—Pilot Tests. Water (Switzerland), 2018, 10, 448.	1.2	2
119	Preparation of a Novel Clay/Dye Composite and its Application in Contaminant Detection. Clays and Clay Minerals, 2019, 67, 244-251.	0.6	2
120	Interactions between Active Ingredient Ranitidine and Clay Mineral Excipients in Pharmaceutical Formulations. Materials, 2020, 13, 5558.	1.3	2
121	Controllable crystal form transformation and luminescence properties of up-conversion luminescent material K <sub>3</sub> Sc <sub>0.5</sub> Lu <sub>0.5</sub> F <sub>6</sub> : Er <sup>3+</sup> , Yb <sup>3+</sup> with cryolite structure. RSC Advances, 2021, 11, 30006-30019.	1.7	2
122	Recent research progress of luminescent materials with apatite structure: A review. Open Ceramics, 2022, 10, 100251.	1.0	2
123	Copper Adsorption Using Hydroxyapatite Derived from Bovine Bone. Advances in Civil Engineering, 2022, 2022, 1-10.	0.4	2
124	Modification of Multilayer Carbon Nanotubes for the Removal of Arsenate. Journal of Nanoscience and Nanotechnology, 2016, 16, 3835-3840.	0.9	1
125	Designing of Birnessite/Polyaniline Composite for Improving Cyclability as Cathode Material for Zinc Ion Batteries Based on Insights into the Reaction Mechanism. ChemistrySelect, 2022, 7, .	0.7	1
126	High Performance Aqueous Li-Ion Flow Capacitor Realized Through Microstructure Design of Suspension Electrode. Frontiers in Chemistry, 2021, 9, 673179.	1.8	0

#	Article	IF	CITATIONS
127	An inorganic thermal insulation material with good performance prepared from obsidian. Magazine of Concrete Research, 2022, 74, 354-363.	0.9	0